

Figure S1. The *CDX2* coding region is disrupted by Crispr targeting (A), resulting in loss of CDX2 protein expression as detected via immunostaining of cells following midgut-directed differentiation (B) or by immunoblotting (C).

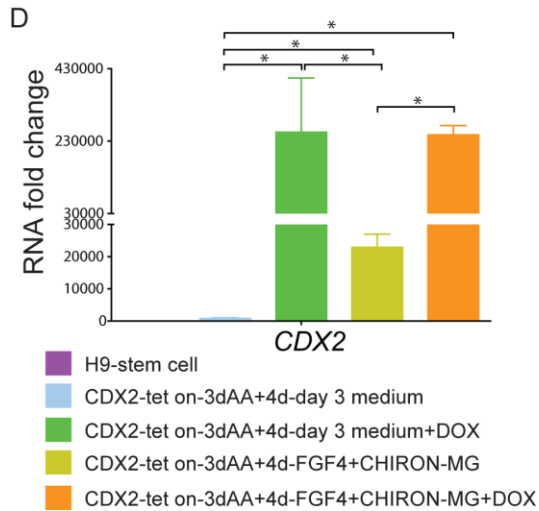
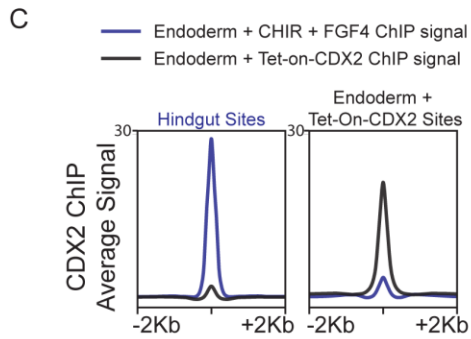
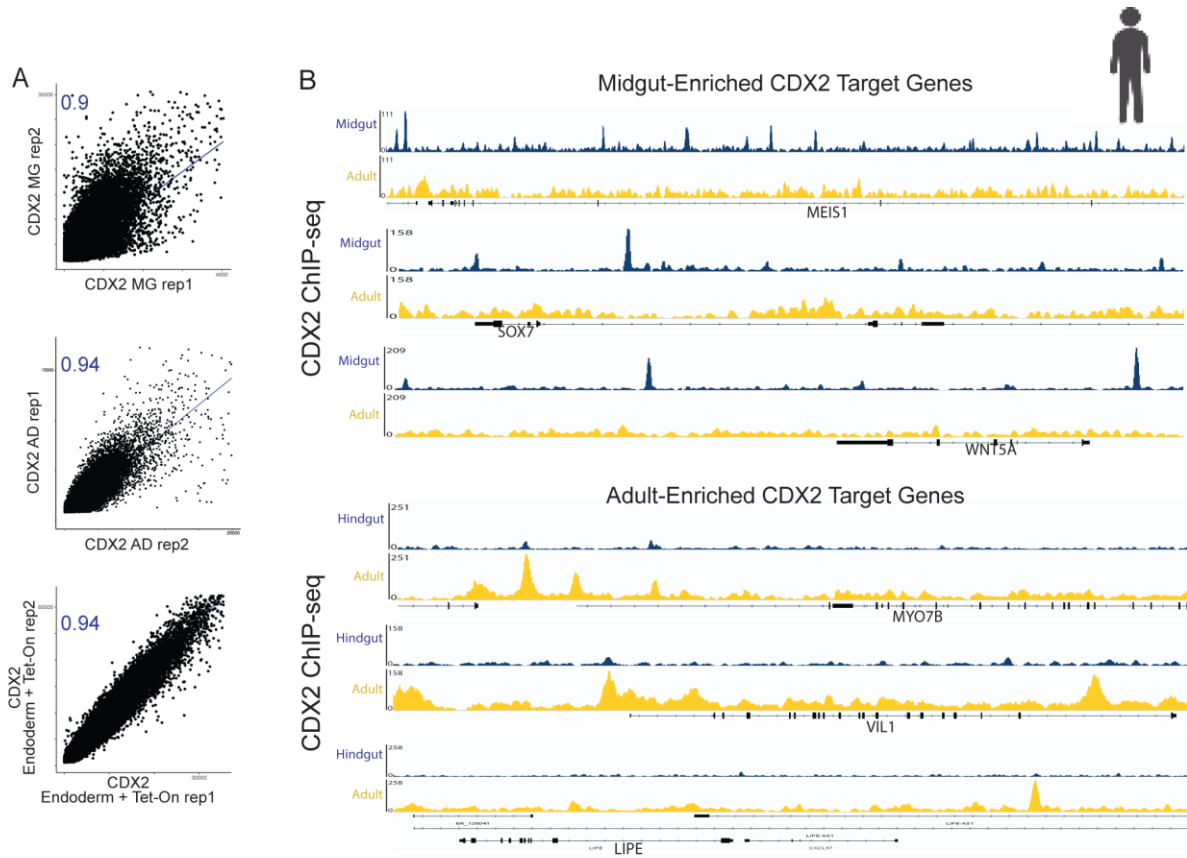


Figure S2. CDX2 has distinct transcriptional targets in the developing midgut versus the adult intestine. A) Pearson Correlation plots indicate consistency between ChIP-seq replicates. (B) Representative examples of CDX2 binding to distinct targets in midgut versus adult intestinal epithelium. C) Average Signal for CDX2 binding at normal midgut sites, versus sites bound by CDX2 only when induced via doxycycline (Ectopic CDX2 sites, Figure 2F). D, *CDX2* transcript levels are robustly induced upon Dox-treatment in the CDX2-tet on cell line, as indicated by qRT-PCR.

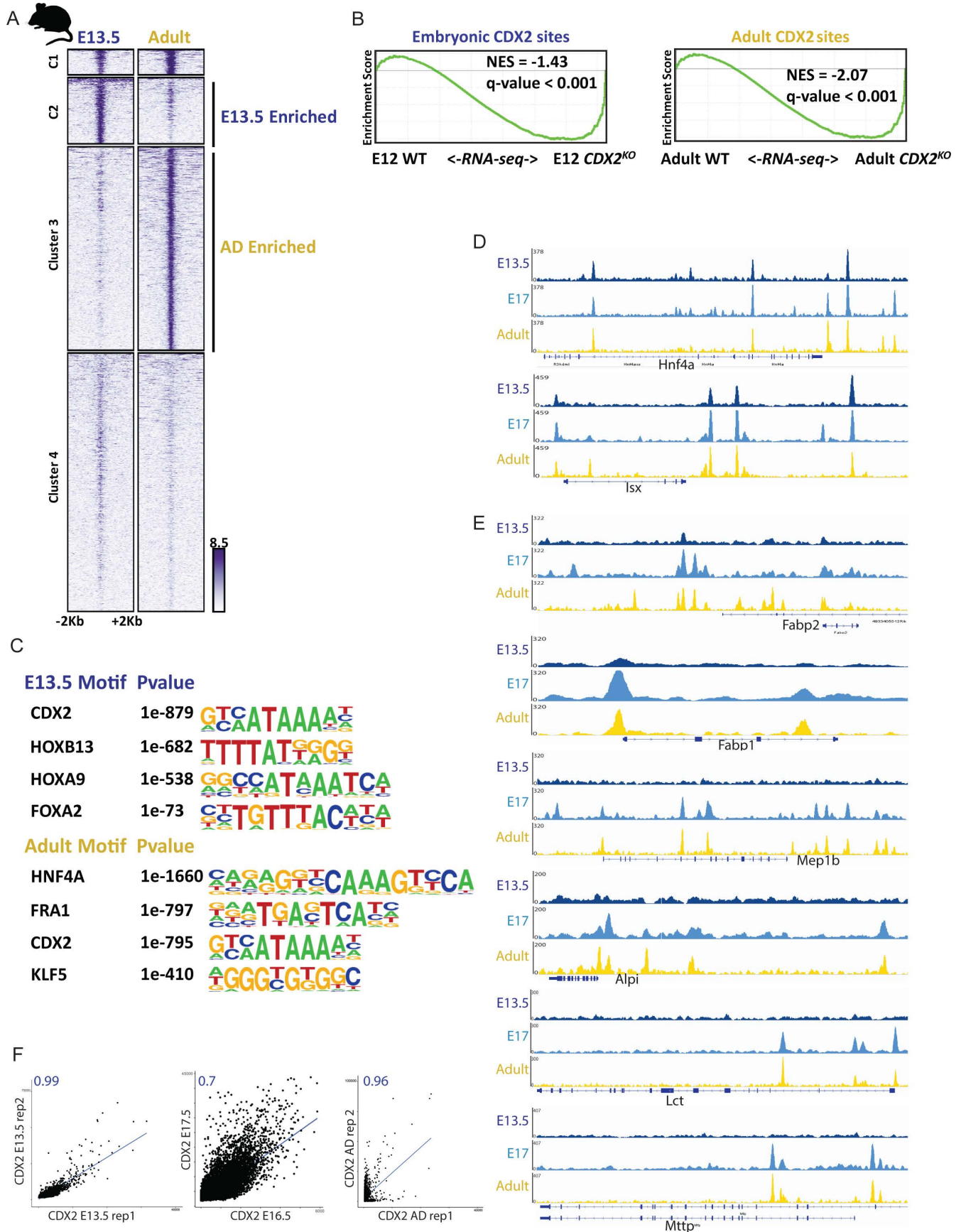
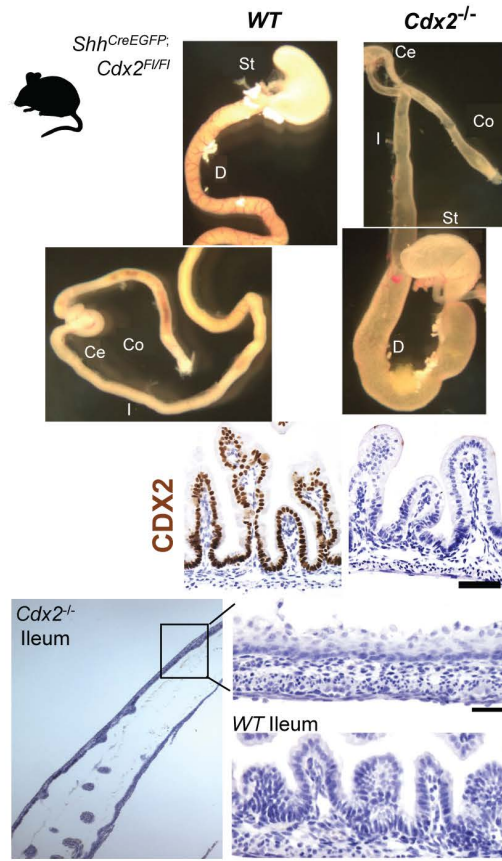
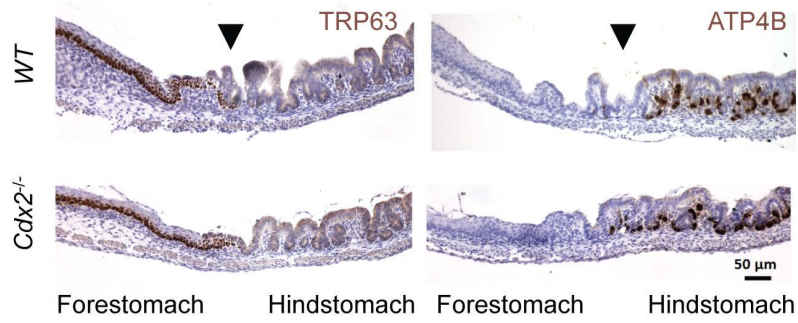


Figure S3. Temporal-specific CDX2 binding is conserved between mice and humans, and impacts intestinal gene expression. A) *k*-means clustering facilitated identification of sites occupied by CDX2 robustly in the intestinal epithelium at either E13.5 or adult stages. B) Genes within 5kb of a condition-specific CDX2 binding site were dependent upon CDX2 for expression, as these genes tend to decrease upon knockout of CDX2 in the embryo (*Shh-Cre; Cdx2<sup>f/f</sup>*) or adult (*Villin-Cre<sup>ERT2</sup>; Cdx2<sup>f/f</sup>*), as measured by RNA-seq. C) Distinct classes of DNA-binding motifs are enriched at CDX2-binding regions unique to the embryo or adult stages, suggesting that CDX2 has distinct partner factors at these developmental stages. D) Examples of persistent, or E) developmental stage-specific, CDX2 binding in the mouse. F) Pearson Correlation plots indicate consistency between CHIP-seq replicates.

A



B



C

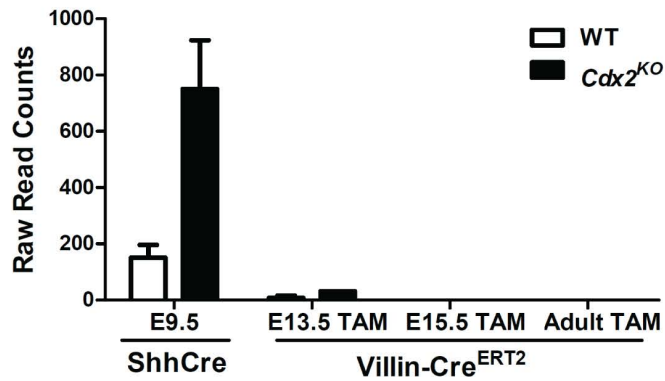
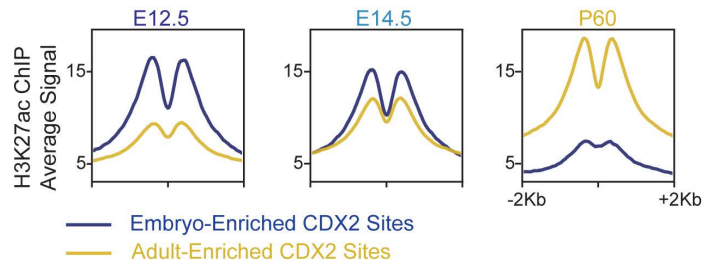
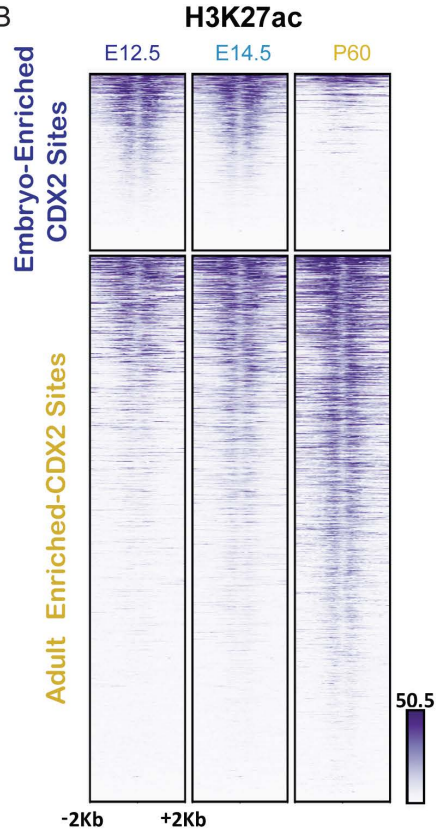


Figure S4. (A) At the top, whole mount images depicting the *Shh*<sup>CreEGFP</sup>;*Cdx2*<sup>ff/ff</sup> phenotype at E18.5. Note the distended intestinal lumen. Below, CDX2 immunostain indicates efficient deletion of *Cdx2*. A closer look at the ileum of the mutants reveals a keratinized squamous appearance in lieu of the simple columnar epithelium present in the control. (B) Control staining of stomachs from *Shh*<sup>CreEGFP</sup>;*Cdx2*<sup>ff/ff</sup> mutants and controls shows the expected pattern of immunoreactivity for TRP63 in the squamous forestomach, and ATP4B in the glandular hindstomach. These stains were done in parallel, and as controls, for those shown in Figure 4. (C) Expression of *Sox2* in intestinal epithelium isolated from mouse intestine at the indicated developmental timepoints and from the indicated *Cdx2* mutant tissues (GSE115541).

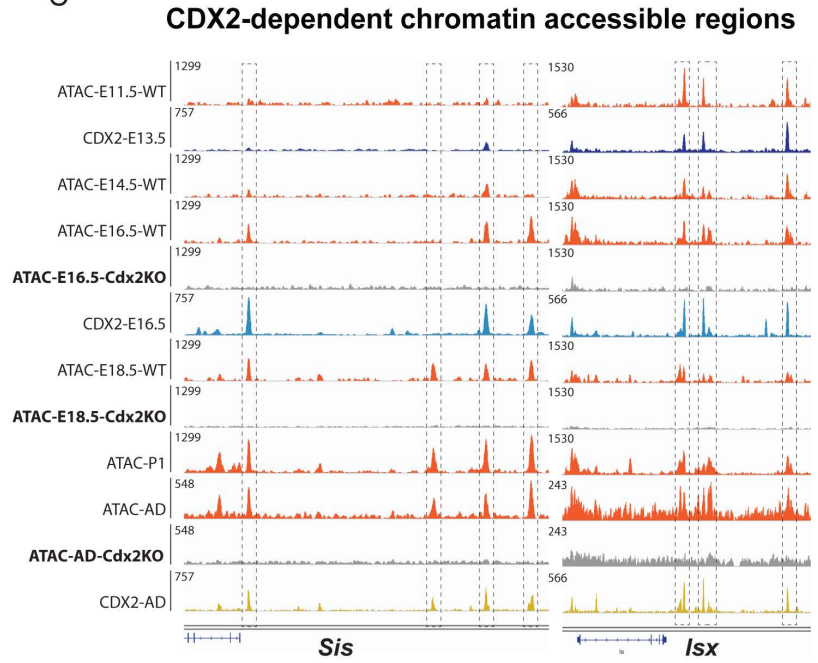
A



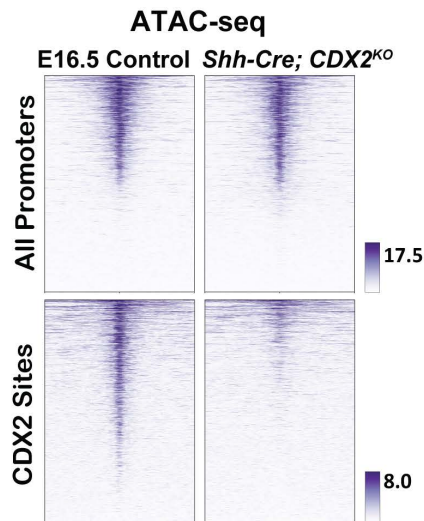
B



C



D



E

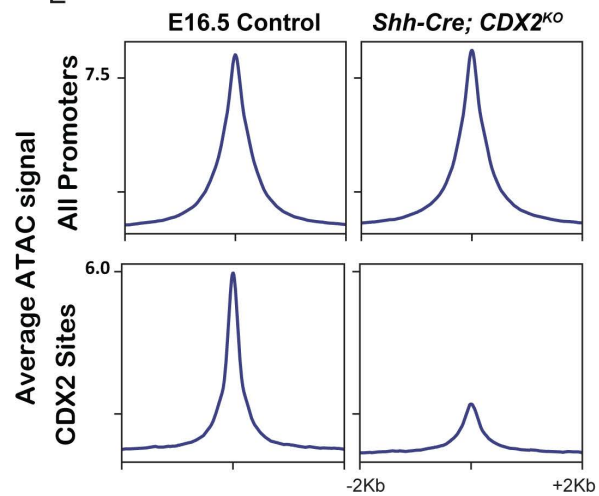


Figure S5. (A-B) Composite plots and heatmaps demonstrating the active chromatin marker, H3K27ac, is enriched at CDX2-binding sites in a stage-specific manner. H3K27ac ChIP-seq data are from (Kazakevych et al., 2017). C) Example data traces of CDX2-binding at accessible chromatin regions over developmental time (ATAC-seq), and their loss of accessibility upon CDX2 knockout using the *Shh-Cre* or *Villin-Cre<sup>ERT2</sup>* (gray tracks). (D-E) Substantial loss of accessible chromatin is observed at CDX2-bound genomic regions in E16.5 *Shh-Cre; Cdx2<sup>ff</sup>* embryos, whereas promoter regions are relatively unaffected.

Table S1. Genome coordinates for CDX2-binding data from CHIP-seq performed in human midgut (Midgut-enriched sites) and Adult (Adult-enriched sites). Additionally, the results of HOMER motif-calling analysis on these sites enriched more specifically in the midgut or adult are reported. Finally, the results of GO term enrichment using DAVID analysis for genes in proximity to these binding regions are reported. These data correspond to findings displayed in Figure 2.

[Click here to Download Table S1](#)

Table S2. CDX2 binding data from CHIP-seq performed in Midgut (Activin, WNT/FGF treatment protocol) versus Endoderm treated with Doxycycline (Activin, Doxycycline-CDX2). Binding coordinates of CDX2 sites found in both conditions (OverlapMidgutTetOn), sites more robustly bound by CDX2 in midgut (MidgutEnriched), or sites more robustly bound by CDX2 when ectopically expressed in endoderm without the midgut-inducing WNT/FGF-treatment (TetOnEnriched) are listed. Additionally, the results of motif-calling analysis of the sites enriched more specifically in the Tet-On or WNT/FGF treated condition are reported. These data correspond to findings displayed in Figure 2.

[Click here to Download Table S2](#)

Table S3. Genome coordinates for CDX2-binding data from CHIP-seq performed in purified mouse intestinal epithelium at E13.5 (Embryo-enriched sites) and Adult (Adult-enriched sites). Additionally, the results of motif-calling analysis on these sites enriched more specifically in the mouse embryo or adult are reported. Finally, the results of GO term enrichment using GREAT analysis for genes in proximity to these binding regions are reported. These data correspond to the findings in Figure 3.

[Click here to Download Table S3](#)